Multi-Point Optimisation of a Propulsion Set as Applied to a Multi-Tasking MAV

Murat Bronz, Jean-Marc Moschetta, Gautier Hattenberger

Multi-Point Optimisation of a Propulsion Set as Applied to a Multi-Tasking MAV

Murat Bronz [*], Jean Marc Moschetta[†], Gautier Hattenberger[‡]
Institut Supérieur de l'Aéronautique et de l'Espace, Toulouse, France
and
École Nationale de l'Aviation Civile, Toulouse, France

ABSTRACT

This study focus on optimisation of electric propulsion system for a given mission with multiple working conditions. A program called *Qpoptimizer* is developed and presented which can analyse and couple numerous motors and propellers from databases for a specific mission. It can also design a custom propeller by using the motor and airfoil databases. *Qpoptimizer* uses *Qprop* and *Qmil* opensource propeller analyses and design programs from Mark Drela. Motor and propeller couples are simulated at each predefined working condition and given a score according to their total performance. This methodology ensures the optimisation of the selected motor and propeller couples to be valid and optimum not only for one working condition (for example: cruise condition) but for all of them (take-off,high speed,etc...). Theoretical models and experimental measurements are explained in order to generate the required databases for the existing motors, propellers and airfoils. Finally, an application of the *Qpoptimizer* program on a real mission is also presented where a custom propeller is optimised according to the weighted mission working conditions.

1 INTRODUCTION

For an electric powered UAV, the motor consumes the biggest percentage of the total energy consumption. This clearly states the importance of optimisation of it. The system approach is the key point on propulsion system optimisation, that is, not only finding the best motor or the best propeller separately, but determining the best motor plus propeller combination.

The mission requirements plays a big role on the selection and optimisation of the propulsion system. These usually consists more than one condition that needs to be satisfied such as take-off and cruise flight. Previous works from T.J.Mueller et al. presents a good example of motor and propeller selection for a MAV [1], but it lacks the identification of each motor and propeller combination's performance evaluation during different phases of the flight since this information can be used as a selection criteria. So in this work, the selection and the optimisation criteria will consider all of the prescribed flight phase (*working conditions*) requirements.

This paper focuses on the optimisation of the propulsion system selection process, for a specific mission with multiple conditions. The new developed *QPOPTIMIZER* program will be presented, which is a motor and propeller coupling program for a large number of input motors and propellers. It uses a set of mission defined working conditions with weighted functions in order to select the best motor and propeller couple for the specific mission. Then the open source programs used in *QPOPTIMIZER* will be explained. Following that, the matching process of motor and propeller couple will be explained including the basics of the electric motor, propeller theoretical models and experimental characterisation test processes.

2 PROBLEM DEFINITION

2.1 Elements of Propulsion System

Electric propulsion system mainly consists of four sub-elements, shown in figure 1; the battery, the motor controller (also called as electronic speed controller, ESC), electric motor and the propeller. A gear system can also be found between the motor and the propeller but mainly it is included in the motor sub-element. Modelisation of the motor and propeller will be explained further in section 4.

[*] PhD Student, muratbronz@gmail.com, murat.bronz@isae.fr
[†] Professor in Aerodynamics, jean-marc.moschetta@isae.fr
[‡] Lecturer in Flight Dynamics, gautier.hattenberger@enac.fr

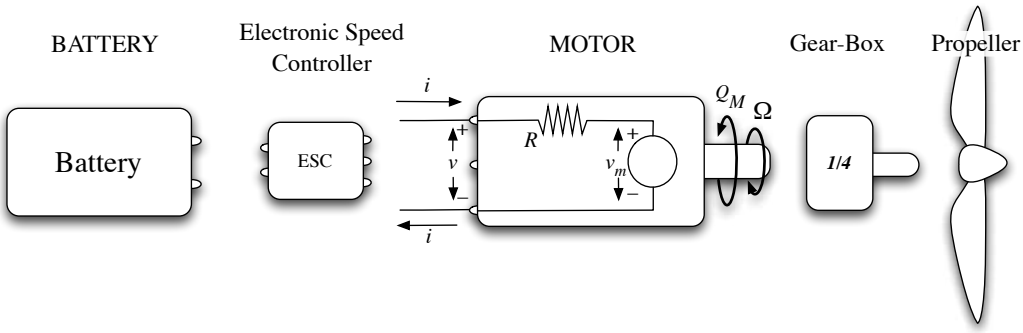

Figure 1: Elements of a generic electric propulsion system.

The electronic speed controller design is out of scope of this thesis, therefore its design will not be included into the optimisation routine, however an efficiency coefficient is included as there exists an effect coming from different brands and types of speed controllers. The same is true for the battery, it is not included in the optimisation routine as they do not have a direct effect on the propulsion system as long as an appropriate type is selected taking into account of its continuous discharge rate. The weight of each element is disregarded in this stage as this makes sense if only when the complete aircraft optimisation is done with the propulsion system included. A conceptual design program, as presented in [2, 3, 4], has to be used as it takes into account the weight of each element while calculating the performance of the aircraft. On this study, the main interest is going to be on the motor and propeller selection.

2.2 Mission Definition

The most important part in the optimisation of the propulsion system is the definition of the mission requirements. Generally it is only the cruise flight conditions which are taken into account while selecting and optimising the motor and propeller selections. In reality, there exists other phases of the flight which the propulsion system has to satisfy additional requirements.

Figure 2 shows several flight phases of an aircraft such as take-off, climb to an altitude, loiter at a constant altitude for surveillance and finally go from point A to B and return at a higher speed for an emergency situation. In each phase of the flight, the aircraft operates at different velocity (V) and thrust (T), the altitude can also be different so that the density will be different (ρ) and the duration of the phase (t) varies according to the mission definition.

Such a flight envelope clearly shows that optimising the propulsion system only for cruise conditions can not be optimum for the overall performance of the aircraft for that given mission. Each phase (will be called as **W**orking **C**ondition) has to be taken into account in the optimisation with its specific variables (T_n,V_n,ρ_n,t_n) in order to achieve an optimum selection for the propulsion system.

Finally, the *Mission Definition* will be described by the *Working Conditions* and their duration time (t). The duration time is only taken as a weight factor here and can be modified if one of the working conditions needs more priority than its duration time compared to the whole mission time.

3 QPOPTIMIZER PROGRAM

QPOPTIMIZER Program is developed in order to select a motor and propeller couple for a given mission definition with multiple conditions as described previously. Numerous motors and propellers from databases can be numerically tested and given a score according to their performance on the defined mission. The mission definition is not only limited with one working conditions, the user can define several working conditions such as in table 1 as previously shown in the figure 2.

	Unit	WC#1	WC#2	WC#3	...	WC#n
Thrust	$[N]$	1.2	1.8	4.5	...	...
Power	$[W]$	0	0	0	...	...
Speed	$[m/s]$	15.0	20.0	3.5	...	...
ρ	$[kg/m^3]$	1.225	1.225	1.225	...	...
WeightFactor	$[-]$	900	150	30	...	...

Table 1: Example of mission working conditions.

These *Working Conditions* mainly act as an objective and also as a constraint in the optimisation process. One can define a **WC** with a weight factor of only 1, relatively low compared to a working condition representing cruise flight with 900 weight factors, so that the program makes sure that the propulsion system satisfies the **WC** but does not give a big score for its performance.

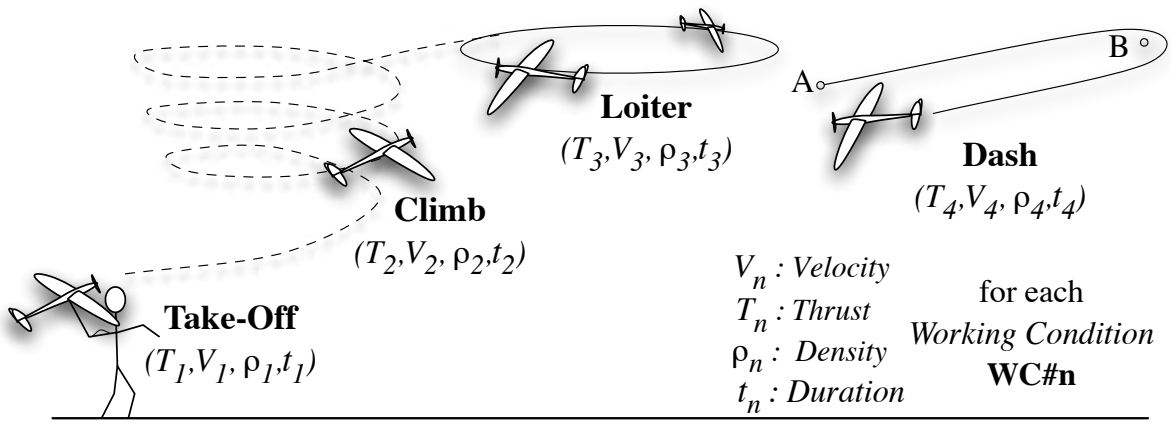

Figure 2: A generic mission definition with multiple flight phases which are called *Working Conditions* (**WC**).

The program uses QPROP and QMIL as its main analyser core and gather their outputs in order to define a score for each motor and propeller couple. This score represents the performance of each motor and propeller couple for the selected mission.

3.1 QPROP and QMIL

QPROP is an open source analysis program for predicting the performance of propeller-motor or windmill-generator combinations. QMIL is the companion propeller and windmill design program which is also open source. Both programs are written by Mark Drela from MIT.

The theoretical aerodynamic formulation is explained in [5]. There, the author remarks that QPROP and QMIL use an extension of the classical blade-element / vortex formulation, developed originally by Betz[6], Goldstein[7], and Theodorsen[8], and reformulated by Larrabee[9]. The extensions include

- Radially varying self-induction velocity which gives consistency with the heavily-loaded actuator disk limit
- Perfect consistency of the analysis and design formulations
- Solution of the overall system by a global Newton method, which includes the self-induction effects and powerplant model
- Formulation and implementation of the Maximum Total Power (MTP) design condition for windmills

QPROP uses three motor specification coefficients (K_v, $\mathcal{R}$, i_0) as an input in order to model the electric motor. For modelling the propeller, it requires the geometry of the propeller which is defined by chord length (c_n)and the pitch angle (β_n) of each spanwise location (r_n) and the airfoil properties which is approximated by a polynomial curve fit as shown in figure 3. This method results with an extremely rapid analyses of motor propeller couples for various conditions.

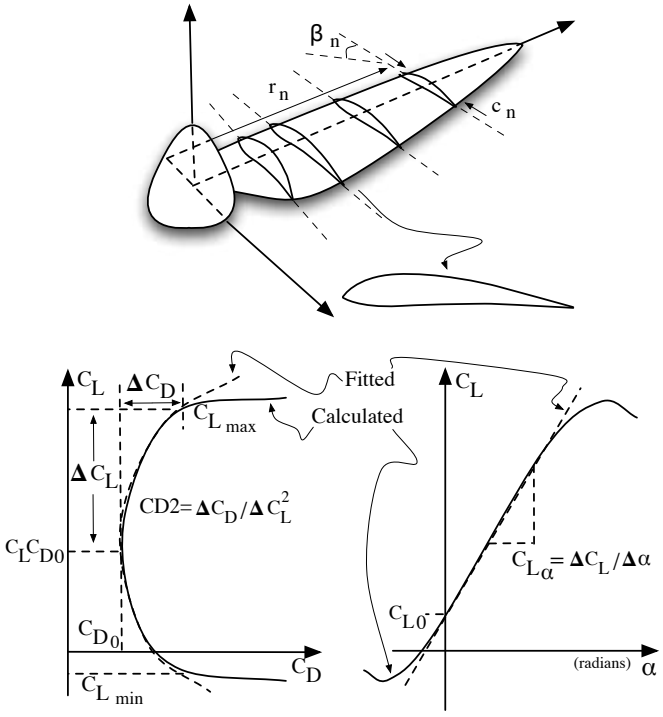

Figure 3: Propeller airfoil coefficients used in QPROP program.

Likewise QMIL requires the working conditions of the propeller that is going to be designed and optimised for. These information include the aerodynamic properties of the airfoil (C_{D_0}, $C_LC_{D_0}$, $C_{L_{min}}$, $C_{L_{max}}$, C_{L_α}, C_{L_0}, $C_{D2_{upper}}$, $C_{D2_{bottom}}$) that is planned to be used,

lift distibution along the span, operating flight speed, desired RPM, diameter and the desired thrust or power generated.

3.2 QPOPTIMIZER Program Flow

QPOPTIMIZER program has two main capabilities. First is to match the most appropriate motor and propeller combination among the motor and propeller databases according to the defined mission requirements. Second is to design the best probable propeller while matching it to the motors from the database. In both cases the final selection is done while taking into account the working conditions and their weight factors. Figure 4 shows the main flow of the program.

The existing motors and propellers are defined with their characteristic coefficients in the corresponding databases. If a custom propeller is going to be designed, then the possible geometry (min and max radius) and RPM envelope has to be defined by the minimum and maximum values that they can get. The mission is mainly defined in the *INPUT* with the working conditions. These working conditions are both used while determining the propeller design conditions and also in the *SIMULATION* phase.

In the *DESIGN* phase, the input file for QMIL is generated according to the mission definition, required working condition specifications and the design envelope which was defined by possible geometry and the RPM minimum and maximum limits. Then QMIL outputs the custom propeller specifications with optimised chord and twisting law.

The MATCH phase simply generates different cases for each possible combination of motor and propeller out of the given propeller and motor databases.

Most important phase is the SIMULATION phase, where each of the motor propeller combination is analysed by QPROP for each of the defined working conditions. After the analyses, each working condition's result is multiplied with its weight factor and finally by summing out all of the working conditions score, a total weighted score is obtained for the motor propeller couple.

An additional FILTER is also defined in order to cancel certain candidates, such as propellers with too low or too high aspect ratios (limited between 3 and 15 as a default) or a maximum weight limit can also be defined (which has to be defined in the INPUT otherwise there is no limitation as a default) for the motor and propeller couple.

An example use of QPOPTIMIZER is explained in section 6 including all the design, manufacturing and test phases. As a brief information, the efficiency of the custom designed propeller was $\%71$ at the defined cruise conditions ($V_{cruise} = 15\,m/s$ and $T_{cruise} = 1.3\,N$) while matching the electric motor's high efficiency working regime ($> \%75$). The total propulsion system efficiency resulted as $\%50$ including the electronic speed controller and the miscellaneous losses (such as cables, connectors...).

4 MODELLING ELECTRIC MOTOR AND PROPELLER

4.1 Electric Motor

Basically, electric motors are electromechanical machines that converts electrical input power into mechanical output power. The general power supply used in the UAVs is DC (Direct Current) so DC motors will be investigated in this chapter. Most common types are brushed and brushless motors. Brushed motors use mechanical and brushless motors use electronic commutation in order to change the direction of electric current and generate a pulling magnetic force between the stator and the magnets.Brushless motors have numerous advantages such as having a higher efficiency than brushed motors, longer lifetime, generating less noise, having higher power to weight ratio. Therefore they are more reliable for the UAV applications. And also they have become more available with the increased interest on radio controlled model aircraft world. Two types of brushless motors exists , In-runner and Out-runner. In the in-runner configuration, the magnets are placed on the shaft of the motor and the windings are at the outer part of the motor. Whereas the out-runner configuration has the magnets turning around the stator. The low inertia of in-runner motor shaft makes them reach to higher rotation speeds compared to out-runner motors. However the out-runner motors commonly preferred for their cooler running and high torque specifications which eliminates the use of additional gear-box.

The important task is to choose the suitable motor for the specified mission requirements. In order to be able to select the correct motor, the characterisation is a must.

First order simplified model using three motor constants, and experimentally obtained characteristics of DC motors will be explained in this section. Figure 5 shows an equivalent circuit model of an electric motor.

As described in [10], the resistance $\mathcal{R}$ of the motor is assumed to be constant and the motor shaft torque Q_m is proportional to the current i according to motor torque constant K_Q. The friction based losses can be

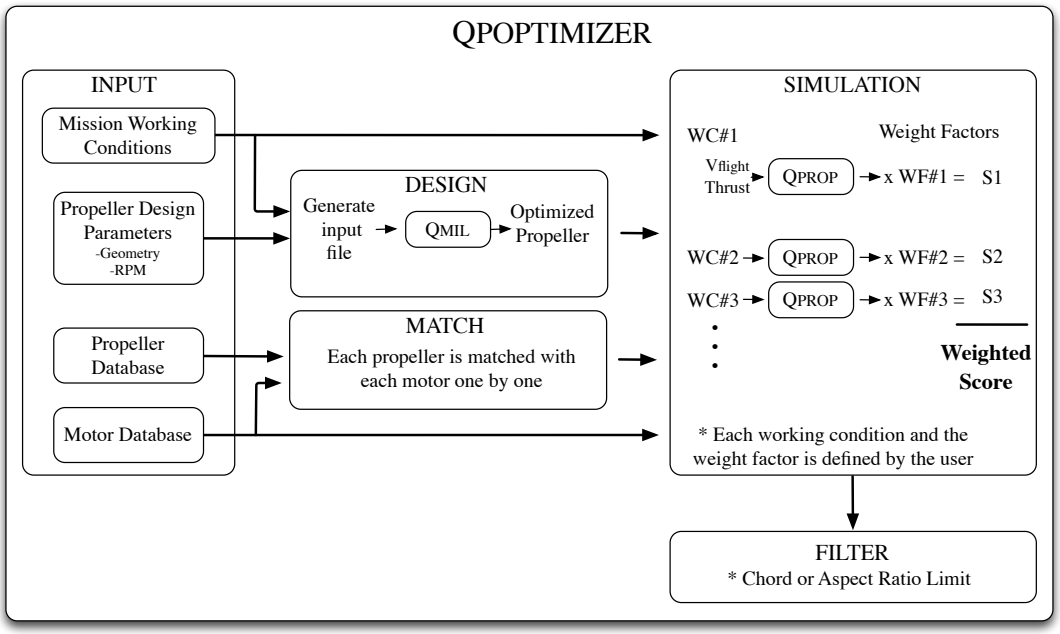

Figure 4: Main flow chart of the QPOPTIMIZER program.

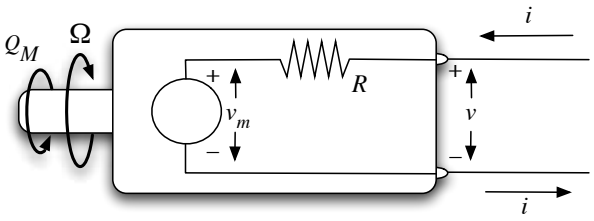

Figure 5: Equivalent circuit for a DC electric motor[10].

represented by the no load current i_0 as a substraction.

$$Q_m(i) = (i - i_0)/K_Q \tag{1}$$

Internal voltage v_m is assumed to be proportional to the rotation rate Ω according to the speed constant K_v of the motor.

$$v_m(\Omega) = \Omega/K_v \tag{2}$$

Then the motor terminal voltage can be obtained by adding the internal voltage and the resistive voltage drop.

$$v(i, \Omega) = v_m(\Omega) + i\mathcal{R} = \Omega/K_v + i\mathcal{R} \tag{3}$$

The above model equations can be rewritten in order to give power, torque, current and efficiency as a function of terminal voltage and rotation rate of the motor. Firstly, the current function is obtained from equation 3.

$$i(\Omega, v) = \Big(v - \frac{\Omega}{K_v}\Big)\frac{1}{\mathcal{R}} \tag{4}$$

Then the others follow ;

$$Q_m(\Omega, v) = [i(\Omega, v) - i_0]\frac{1}{K_Q} = \Big[\Big(v - \frac{\Omega}{K_v}\Big)\frac{1}{\mathcal{R}} - i_0\Big]\frac{1}{K_Q} \tag{5}$$

$$P_{shaft}(\Omega, v) = Q_m\Omega \tag{6}$$

$$\eta_m(\Omega, v) = \frac{P_{shaft}}{iv} = \Big(1 - \frac{i_0}{i}\Big)\frac{K_v}{K_Q}\frac{1}{1 + i\mathcal{R}K_v/\Omega} \tag{7}$$

As a reminder, K_v is usually given in RPM/Volt in motor specifications, however here it is taken as rad/s/Volt and K_Q is taken in Amp/Nm. It should be also noted that $K_Q \approx K_v$.

By knowing the first order motor constants $(K_v, K_Q, i_0, \mathcal{R})$ of any off the shelf motor, the theoretical characteristic plots can be obtained by using above equations. General view of the motor outputs are shown in figure 6.

4.2 Experimental Motor Characterisation

In order to characterise the electric motors experimentally, the test bench which is shown in figure 7 is used. The motor is fixed on a free turning axe supported with ball bearings, and a torque sensor limits the turning of this axe in order to measure the torque generated by the motor while running. The calibration of the thrust

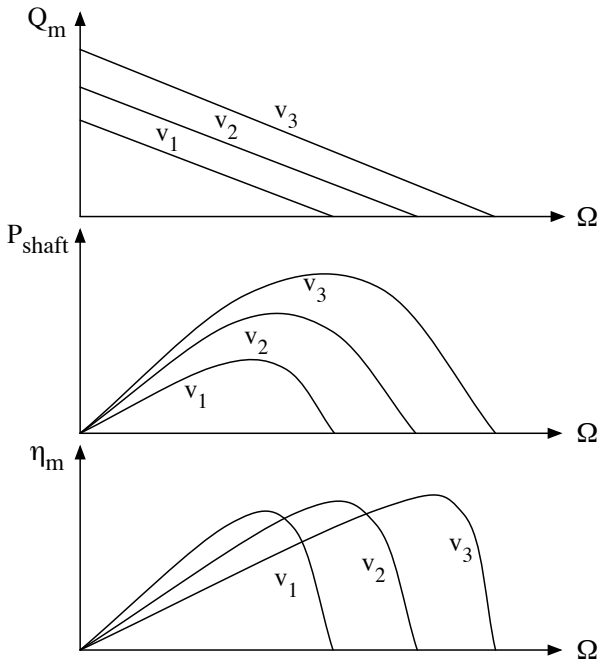

Figure 6: Theoretical motor outputs versus motor rotation rate for different input voltages.

and torque load-cells are done by using traditional pulleys with known loads attached on to them with thin rigid ropes. The load sensor(V018-113) that is used for the torque measurements was limited to $0.5\,N$ where the load arm was applied from $8\,cm$ from the centre of the rotation axis of the motor resulting with a $4\,Ncm$ limit. The thrust axis uses a $20\,N$ limited load cell and calibrated by using $50\,gr$ increments with the pulley. An optical speed sensor located near the motor measures the rotation speed. The power supply that is connected can directly record the voltage and the current consumed by the motor. Finally, all these sensors are integrated in a synchronised way in *Labview*[1] program.

The key point is to generate variable resistance for the motor while running on a *constant voltage*. Figure 8 shows the wheel that is used for this purpose. Simply, an air supply is used in order to generate a breaking force on the motor and the flow rate of the air supply is increased in order to cover all of the working envelope of the motor. By this way the whole characteristics of the motor for a given voltage input can be viewed. The procedure is repeated for different voltages and the whole performance characteristics are extracted.

The characterisation of the motor can also be done by other methods such as using a second motor connected to the shaft of the first one in order to generate and vary

[1] http://www.ni.com/labview/

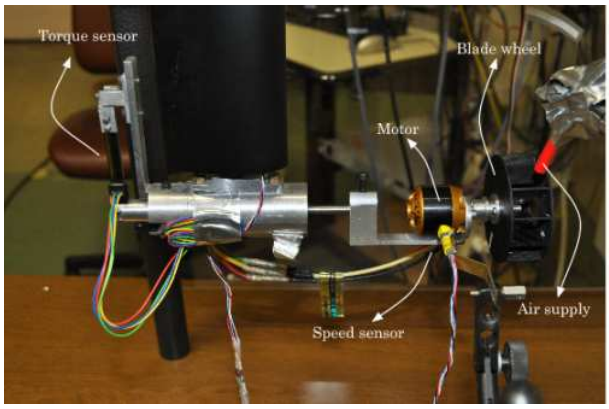

Figure 7: Motor test bench.

the resistance load or a magnetic breaking system can be implied which will result with a higher precision on the resistance change. However the simplicity of using an air break at the moment of the tests outweighed all of the possible the disadvantages.

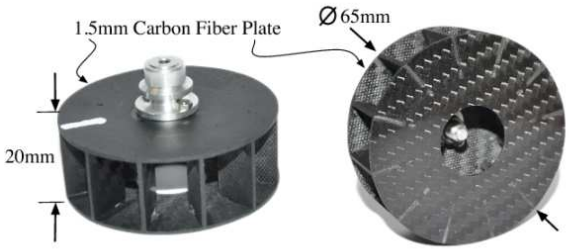

Figure 8: The wheel that is used in motor characterisation.

Figure 9 and 10 shows the comparison of performance curves that are measured experimentally and calculated with the previously explained theoretical model for AXI 2212-20 motor.

It can be seen that the simple model has an error of approximately 5% on average. As a conclusion, this theoretical and experimental match shows that in the absence of experimental testing of the electric motors, the characteristic specifications which are given by the manufacturer can be used for the initial selection of the motor.

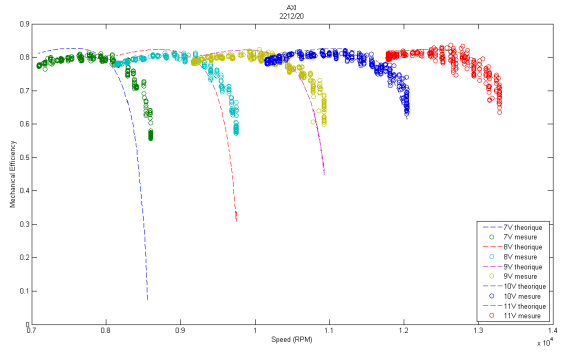

Figure 9: AXI 2212-20 Theoretical and experimental mechanical efficiency curves versus rotation rate for various input voltages.

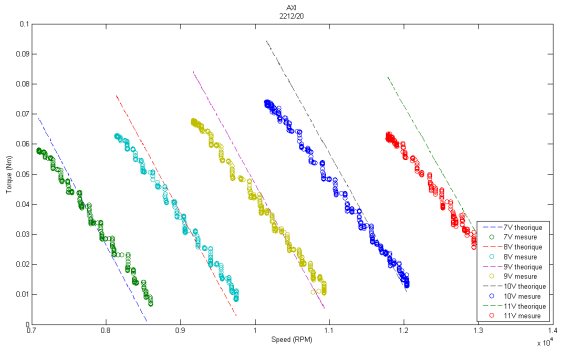

Figure 10: AXI 2212-20 Theoretical and experimental shaft torque curves versus rotation rate for various input voltages.

4.3 Propeller

The propeller is a rotating wing which utilises the mechanical power input in order to accelerate the air particles to generate thrust.

The basics of characterisation of the propeller is going to be explained here, however a deeper explanation can be found in [11]. The thrust and power coefficients are used to characterise a propeller, which depend on the advance ratio λ, the average blade Reynolds number Re, and the geometry of the propeller.

$$C_T = C_T(\lambda, Re, geometry) \tag{8}$$

$$C_P = C_P(\lambda, Re, geometry) \tag{9}$$

Reynolds number of the propeller is defined according to its average chord length c_{ave}

$$Re = \frac{\rho\,\Omega R c_{ave}}{\mu} \tag{10}$$

Advance ratio λ is also well known as J in most of the literature.

$$\lambda(\Omega, V) = \frac{V}{\Omega R} \tag{11}$$

$$\lambda(\Omega, V) = J(\Omega, V) = \frac{V}{nD} \tag{12}$$

where n is,

$$n = \frac{\Omega}{2\pi} \tag{13}$$

Thrust and torque of the propeller as a function of rotation speed and the velocity,

$$T(\Omega, V) = \frac{1}{2}\rho(\Omega R)^2\,\pi R^2\,C_T = \frac{1}{2}\,\rho V^2\,\pi R^2\frac{C_T(\lambda, Re)}{\lambda^2} \tag{14}$$

$$Q(\Omega, V) = \frac{1}{2}\rho(\Omega R)^2\,\pi R^3\,C_P = \frac{1}{2}\,\rho V^2\,\pi R^3\frac{C_P(\lambda, Re)}{\lambda^2} \tag{15}$$

Finally, the efficiency of the propeller is,

$$\eta_{propeller}(\Omega, V) = \frac{T(\Omega, V)V}{Q(\Omega, V)\Omega} = \frac{C_T}{C_P}\lambda \tag{16}$$

4.4 Typical Propeller Performance Curves

Typical propeller performance plots η, C_T and C_P versus advance ratio are shown in figures 11,12 and 13 [12]. The curves in the figures are for the same chord distribution and twisting law but with various root pitch angle, which is commonly seen on variable pitch propellers.

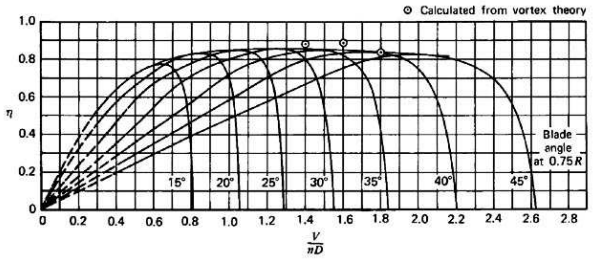

Figure 11: Typical propeller efficiency curves as a function of advance ratio **J**.

4.5 Experimental Propeller Characterisation

The same test bench which has been shown in section 4.2 is also used for the experimental characterisation of the propellers. Instead of the resistance generating wheel, the propellers that are going to be tested, are mounted to the test bench. Rotational speed, torque and the thrust of the propeller is measured at different wind tunnel speeds. Test bench is shown in figure 14.

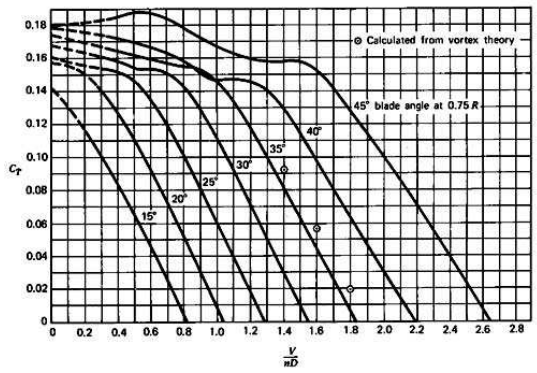

Figure 12: Typical propeller thrust curves as a function of advance ratio **J**.

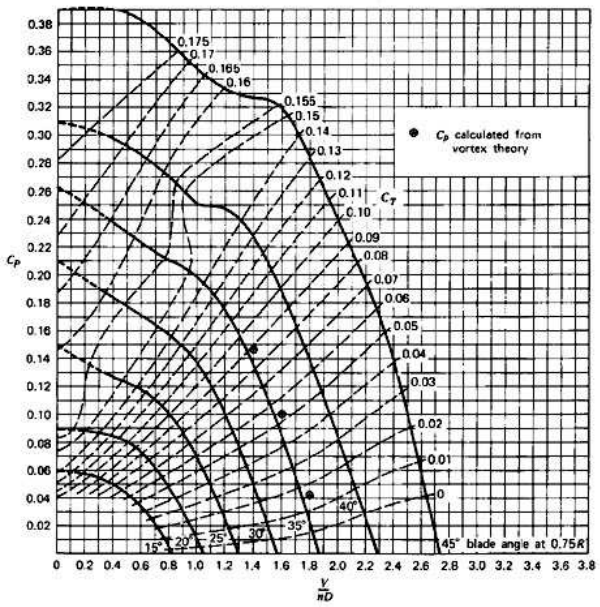

Figure 13: Typical propeller power curves as a function of advance ratio **J**.

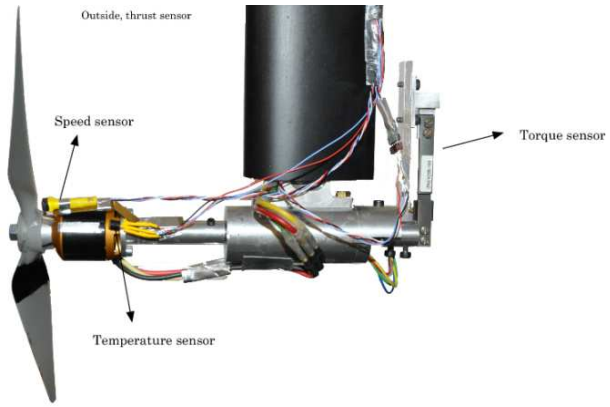

Figure 14: Propeller test bench.

5 Motor and Propeller Matching

Regardless of its maximum efficiency of an electric motor or a propeller, if they are not matched correctly for the given mission specifications, the resultant total efficiency will be poor. The theoretical and the experimental characterisation of the electric motors and the propellers have to be used in order to match the motor and propeller couples. Figure 15 explains the matching process with steps.

The mission requirements states the *Thrust* (T_p) (Step 1) needed at a certain flight speed *V* for the propeller, according to propeller's thrust versus rotation speed characteristic curve , the corresponding rotation speed (Ω) is found (Step 2). The rotation speed at the given flight speed *V* will determine the efficiency of the propeller (η_p) (Step 3). In optimal case, the efficiency peak of the propeller should roughly correspond to the given rotation speed. Then the torque of the propeller Q_p defined for the given flight speed is plotted and the torque value corresponding to the rotation speed (Ω) is found (Step 4). In order to match the motor and the propeller's torques ($Q_m = Q_p$) , the required voltage of the motor is calculated (v) (Step 5). The resultant voltage and the rotation speed of the motor gives the efficiency point, η_m, where the motor works (Step 6). Finally, the multiplication of the motor and the propeller efficiencies gives the total propulsion set efficiency(speed controller efficiency has to be added separately). If the motor's efficiency is on the peak region, then the matching can be defined as good. Otherwise, a gear can be used to shift the peak efficiency region of the motor in order to match with the propeller's rotation speed. The explained method has already been built-in the QPROP program.

6 Application of Qpoptimizer

As explained in section 3.2 the most important input is the working conditions which is defined by the mission itself. The final performance criteria is also going to be evaluated according to these working conditions and their weight factor which implies the importance of each working condition.

6.1 Working Conditions

The first calculations and later the wind tunnel test of the aircraft, *SPOC*, that is designed for the long range mini UAV project showed that the thrust needed at cruise speed is around $1.3\,N$. This condition created the first working condition and as the main flight is going to

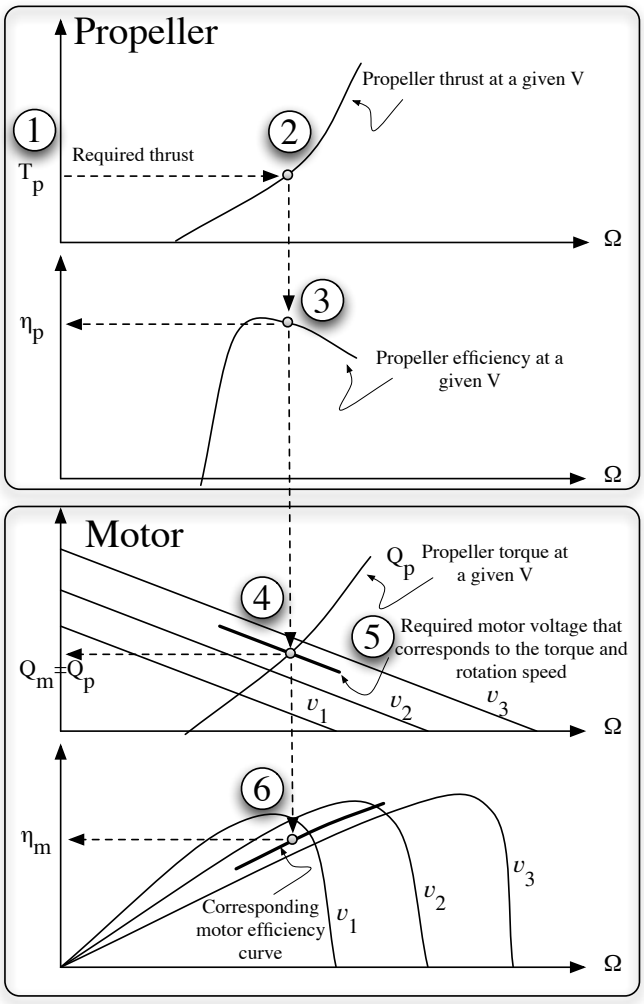

Figure 15: Motor and propeller matching procedure as explained in [11].

be almost flown in this condition, the weight factor has been selected to be 70 for it. In the time of this custom propeller design phase, the first flight tests of the *SPOC* was already accomplished. There, the need of an instant climbing ability has seen to be required. Constant climb with $2\,m/s$ vertical speed requires $3\,N$ of thrust at $15\,m/s$ flight speed for *SPOC*, this condition created the second working condition. The weight factor is selected to be 10 as it is not that much significant for the final mission performance, the important thing is to be able to achieve that condition. As the last condition, the stall phase has been selected, from the wind tunnel tests, it is known that the stall speed for *SPOC* is around $11\,m/s$ and the required equilibrium thrust is $1.4\,N$, given with a really small weight factor of 5, the third working condition has been created. The sum of the weight factors do not necessarily need to be 100, they are normalised within the program. The table 2 show all of the selected working conditions for QPOPTIMIZER.

	Unit	WC#1	WC#2	WC#3
Thrust	$[N]$	1.3	3.0	1.4
Speed	$[m/s]$	15.0	15.0	11.5
WeightFactor	$[-]$	70	10	5

Table 2: Mission working conditions of the *SPOC* UAV.

6.2 Motor Database

The ability of using a big motor database in QPOPTIMIZER gives a big freedom on choosing motors but in the content of the project there was only two motors to be used while designing the optimised propeller. These motors are selected according to their experimental bench test results and finally the fuselage of the *SPOC* is optimised according to the use of these motors. They are AXI 2212-26 and AXI 2217-12. Another important reason why these motors were chosen for the project is the rapid availability of them for the school.

6.3 Airfoil Selection

The airfoils that are going to be used in the propeller design needs to be defined in the inputs for QPOPTIMIZER. The definition is simply done by a polynomial curve fit to the aerodynamic characteristics plot of the airfoil, which are drag coefficient versus lift coefficient and lift coefficient versus angle of attack plots.

Some off the shelf propellers were already experimentally tested previously at the cruise speed and required thrust. These tests gave an approximate value about the average chord reynolds number of the propeller which is around 60000. Additionally, the dominance of thin cambered airfoils in the low reynolds conditions is shown in several work [**?**]. Firstly, some existing thin airfoils have been searched through the internet databases [2] and M.Selig's books [13, 14, 15]. The comparison is made between 60000 and 100000 reynolds number regime, also a smooth stall and consistent drag change versus lift is considered as selection criterias. After some investigation, five airfoils are selected as candidates, BE-50, GOE-417a, BW-3, CR-001 and GM-15.

One of the most important criteria while airfoil selection was the manufacturability. As we already selected a computer assisted numerically driven CNC milling machine manufacturing with moulds, controlled variation of thickness along the chord was achievable. This gives the opportunity of selecting better performing airfoils

[2] UIUC, http://www.ae.illinois.edu/m-selig/ads.html

rather than curved constant thickness (plate like) airfoils. As a next step, a custom airfoil is designed fulfilling a wider range of lift regime. The five candidate airfoils and the designed MBP-006 airfoil geometries and their aerodynamic characteristics are shown in figure 16.

For our application, the best suited airfoil among the first five selected candidates was BE-50, because of its smoother behaviour around $Cl = 1.0 - 1.2$ and lower drag value at corresponding smaller lift coefficients than 1.0. All the other airfoils have a sudden peak of change in drag coefficient, and also have higher drag coefficient at lift coefficients that are lower than 1.0.

BE-50 is taken as the reference airfoil to start the design with XFOIL. The objective was to improve the already existing good characteristics and work on the lower lift coefficient part. In order to smooth the high lift coefficient regime a little bit more and reduce drag coefficient around $Cl = 0.2 - 1.0$ lift coefficient regime, maximum lift coefficient is compromised.

The resultant MBP-006 airfoil has $\%10$ less maximum lift coefficient but performs smoother in overall. Ideally, the required thrust should stay almost constant over the entire flight, but it is already known from the previous tests that there will be fluctuations on the required thrust while controlling the aircraft. Obtained reduced drag around $Cl = 0.2 - 1.0$ regime becomes very important for the airfoil performance of the propeller and makes it more optimised in a practical way.

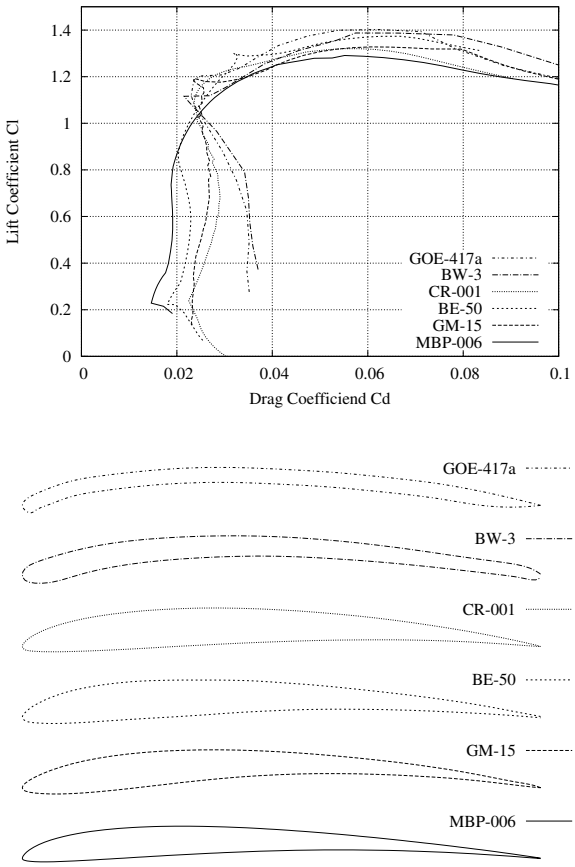

Figure 16: Selected airfoils and their lift versus drag coefficient plot calculated by XFOIL for 60000 Reynolds number.

7 RUN CASES

The two motors which are selected for the project previously, were AXI2217-12 and AXI2212-26. The bench test results showed that there is a significant difference between the expected theoretical performance and the experimental performance of AXI2217-12, the theoretical performances are almost $\%10$ overestimated than the experimental ones. The performance plots are shown in figure 17 and 18. As an additional to this, there is an $13g$ of weight penalty for AXI2217-12 as it is a bigger motor than AXI2212-26. Being a bigger motor also means that the throttle percentage is going to be low while cruise flight conditions, so that the speed controller efficiency will be lower than expected for this case as well. The only advantage is going to be the additional maximum thrust value for safety reasons. Taking into account all these facts, the design of the new propeller is selected to be made primarily for the small AXI2212-26 motor and try to have the bigger AXI2217-12 motor for some critical test flight where the additional power can be necessary.

As an input, the RPM and propeller tip radius ranges must be defined in order to run the simulations. The precision of the optimisation is defined by the step of both parameters. Table 3 shows the selected envelope for the design.

Spanwise location	Minimum	Maximum	Step
RPM	2000	12000	50
Tip radius $[mm]$	10	200	1

Table 3: Parameters used for the optimization

Additionaly, the desired spanwise lift coefficient distribution required to be defined for QPOPTIMIZER (QMIL program needs this information). Two spanwise C_L distributions were tested and are shown in table 4.

Previously selected working conditions, shown in

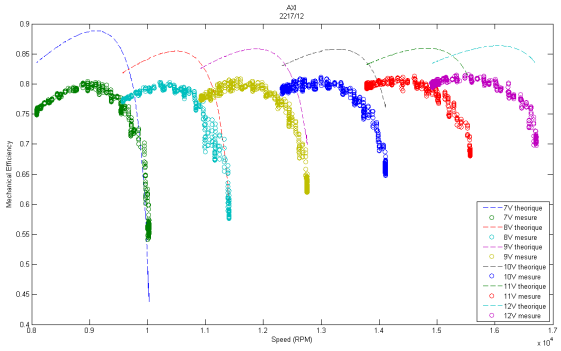

Figure 17: AXI 2217-12 theoretical and experimental mechanical efficiency curves versus rotation rate for various input voltages, showing the significant difference between the theoretical and experimental test results.

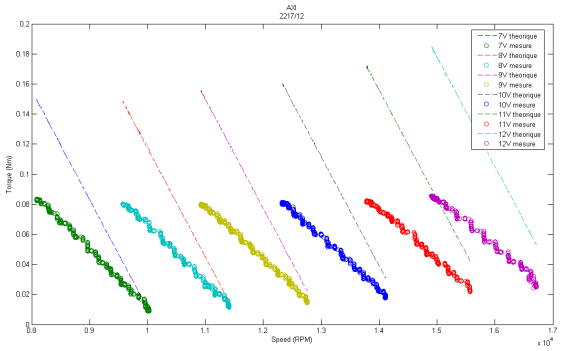

Figure 18: AXI 2217-12 theoretical and experimental shaft torque curves versus rotation rate for various input voltages, showing the significant difference between the theoretical and experimental test results.

table 2, used for every run case. As a common result in every run case, the higher C_L distribution gave better performances. The table 5 shows the best results of all the run cases. C_L1 distribution is selected to be used for the final design.

The resultant global efficiency is higher using the bigger AXI2217-12 motor as expected. As it is already known that the AXI2217-12 is over estimated for the efficiency and also heavier, the small AXI2212-26 motor fits more appropriately for our application.

A monoblade propeller was also designed using the same approach. Demanding the same thrust with only one blade created a propeller with wider chords. This improved the overall airfoil efficiencies along the span because of increased Reynolds number. The best estimated overall efficiency for the motor and monoblade

Spanwise location	0.10	0.50	1.00
C_L distribution 1	0.75	0.65	0.40
C_L distribution 2	0.60	0.45	0.40

Table 4: Lift coefficients distributions

		Cruise efficiency	RPM	Tip radius $[cm]$
AXI2212-26	C_L1	59.5%	5800	11
AXI2212-26	C_L2	58.9%	5700	11.5
AXI2217-12	C_L1	63%	5000	12.5
AXI2217-12	C_L2	61.9%	5000	12

Table 5: Best global efficiencies of the motor and propeller couples for the cruise conditions are shown (note that the speed controller losses are not included).

propeller couple is calculated as 62.6% by QPOPTIMIZER. Unfortunately, because of the limited time span of the project and the expected possible problems that could come with a monoblade propeller cancelled the investigation of the monoblade concept and the manufacturing continued with the bi-blade propeller design.

8 Manufacturing

The manufacturing of the propeller is decided to be done in house, in composite laboratory of ISAE. Thinking about each landing phase of the tests flights and having no landing gear on the SPOC plane, the propeller was in danger of breaking while landing. In order to prevent this, the hub of the propeller is designed for a folding root, and finally a custom spinner is also build in the exact needs of SPOC plane. Figure 19 shows the integration of the folding blade with the spinner.

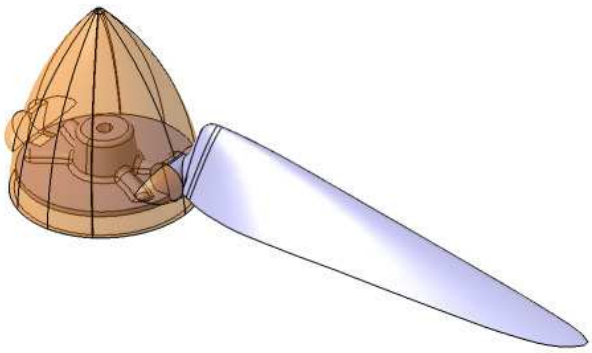

Figure 19: Designed propeller and its spinner's CATIA drawing.

Moulds are designed in Catia V5 and manufactured with CNC milling machines in order to achieve the necessary precision. Each blade is build out of three piece of moulds, top, bottom and the folding axis pin. The

spinner cone is build by using six pieces of moulds, two sides, two folding axe pins and two prop blade root inserts. Finally the base of the cone is build by using three moulds, top bottom and the rotation axis pin. The spinner cone and the base moulds are designed to fit each other in order to maintain the base to the cone in the same rotation axis perfectly to prevent any possible balance problems.

The propeller was made of carbon fibre. The material was chosen because of its low weigh and its high strength. The required pieces are first cut into shape and then wet lay-up is done by hand into the moulds. Different orientations ($45°$ and $90°$) of carbon fibre woven were used on the skin for the torsional strength of the propeller. Additionally, unidirectional carbon fibre mesh were placed in order to sustain the bending forces of the blade. As the propeller blade has a specific airfoil, a certain amount of material should have filled the thickness. The exact required material quantity is found by trial and error as the weight of each blade was only $1.5\,g$. There was no need to use vacuum bagging process as the two mould halves completely fits onto each other.

The spinner cone is also build by wet lay-up by hand, in order to achieve a smooth surface and fix the layer on the skin of the cone, a balloon is inflated inside the cone. A silicon insert should have given better results but this method is used because of the time restrictions. The figure 20 shows the resulting cone and its molds.

Figure 20: The cone and its molds

Finally after manufacturing two blades, spinner cone and the base, they are integrated into each other to form the custom designed propeller. The figure 21 shows the resulting propeller. The fixation of the spinner to the motor shaft is done internally. First the two blades should have removed and then the inner fixation screws that are placed on the spinner base plate can be reached. This method makes the fixation a little bit complex but once it is fixed there will not be any gap between the spinner and the nose of the plane or any protruding screws that can create additional drag.

Figure 21: The resulting custom propeller

9 Test Results

The propeller test bench which is shown in section 4.3 figure 14 is used for the tests. The main point of interest was to measure the performance at cruise conditions which are $15\,m/s$ of flight speed and $1.3\,N$ of thrust generation. Additionally, as expected from the theoretical calculations, the propeller has to have more than $4\,N$ of thrust at this flight speed at full throttle. Figures 22 and 23 show the global efficiency (speed controller + motor + propeller) and propeller efficiency alone versus thrust generated at $15\,m/s$ flight speed condition. It can be seen that the propeller efficiency is around 71% at cruise condition thrust, and the final global efficiency is around 50% which includes the speed controller, motor and the propeller. The maximum thrust measured at full throttle was $4.25\,N$ at $15\,m/s$ speed.

Expected global efficiency was 59.5% however, the measured efficiency was only 50%. The assumptions and the simplifications that is done in theoretical calculations will cause a difference between the real world and the calculations, but there are also several reasons that cause difference. First of all the theoretically assumed 59.5% efficiency does not take into account the speed controller, which usually have around 95% of maximum efficiency. Additionally, the designed spinner could not have used in the wind tunnel tests because of the additional pressure drag that it generates without having the real fuselage behind it. Instead of spinner, an aluminium piece is manufactured in order to hold the two folding propeller blades together in the wind tunnel, there is additional drag coming from this piece resulting with lower efficiency. Finally the manufactured airfoil shape and the propeller geometry could have differ from the designed and analysed one which results normally reduction on the expected efficiency as well.

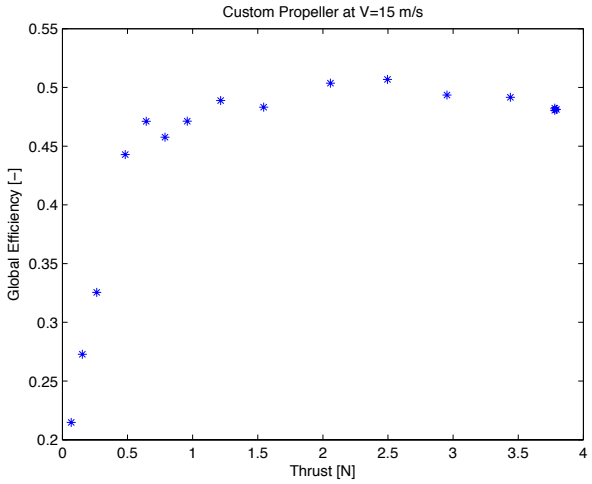

Figure 22: The global efficiency versus Thrust [N] plot for the custom designed propeller at $15\,m/s$ speed.

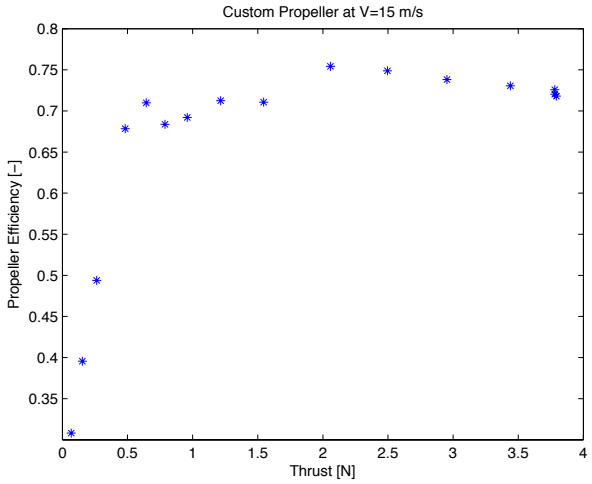

Figure 23: The propeller efficiency versus Thrust [N] plot for the custom designed propeller at $15\,m/s$ speed.

10 Conclusion

A multi-point optimisation methodology and a devoted program called QPOPTIMIZER is introduced for matching and designing electric propulsion system. The importance of the mission definition and optimisation of the propulsion system according to multiple working conditions is highlighted. The modelling of the motor and propeller is described stating the importance of the accuracy of the models. The motor and propeller matching procedure is explained deeply.

Finally, the proposed program is used in designing a custom propeller for a real life application for a mini-UAV that has to fly a long range mission. The results showed that the program correctly matches the motor and propeller's individual peak efficiency regions optimised while taking into account every working conditions. This leads to an optimum selection of the propulsion system. However, the resultant performance values are a little bit optimistic ($\%5 - 10$ for the complete propulsion system) compared to the experimental measurements which has been previously expected.

Acknowledgement

The authors would like to thank Prof. Mark Drela for sharing his great work QPROP and QMIL within the GNU v2 licence which makes it possible to use them as the core aerodynamic analyser programs of the QPOPTIMIZER. Also we would like to thank a lot Xavier Foulquier and Guy Mirabel for their precious helps and advices for the composite manufacturing.

The realisation of the custom propeller would not be possible without the work that has been done by Miguel Morere Y Van Begin, Guillaume Soete, Pierre Joachim and Benjamin Fragniére(aka. The Belgium Beatles). Finally, this study has been co-funded by the European Union. Europe is involved in Midi-Pyrénée with European Fund for regional development.

References

[1] Thomas J. Mueller, James C. Kellogg, Peter G. Ifju, and Sergey V. Shkarayev. *Introduction to the Design of Fixed-Wing Micro Air Vehicles*. American Institute of Aeronautics and Astronautics,Inc., Virginia,VA, 2007.

[2] Murat Bronz, Jean-Marc Moschetta, Pascal Brisset, and Michel Gorraz. Towards a Long Endurance MAV. In *EMAV2009*, Delft, Netherlands, September 2009.

[3] Murat Bronz, Jean-Marc Moschetta, Pascal Brisset, and Michel Gorraz. Towards a Long Endurance MAV. *International Journal of Micro Air Vehicles*, 1(4):241–254, 2009.

[4] Murat Bronz, Jean-Marc Moschetta, and Pascal Brisset. Flying Autonomously to Corsica : A Long Endurance Mini-UAV System. In *IMAV2010*, Braunschweig, Germany, July 2010.

[5] Mark Drela. *QPROP Formulation*. MIT Aero and Astro, June 2006.

[6] A.Betz. Airscrews with minimum energy loss. Technical report, Kaiser Wilhelm Institute of Flow Research, 1919.

[7] S.Goldstein. On the vortex theory of screw propellers. In *Proceedings of the Royal Society*, volume 123, 1929.

[8] Theodore Theodorsen. *Theory of Propellers*. McGraw-Hill, New York, 1948.

[9] E.E Larrabee and S.E. French. Minimum induced loss windmills and propellers. *Journal of Wind Engineering and Industrial Aerodynamics*, 15:317-327:317–327, 1983.

[10] Mark Drela. First-order dc electric motor model. Technical report, MIT, Aero and Astro, February 2007.

[11] Mark Drela. Dc motor and propeller matching , lab 5 lecture notes. Technical report, MIT, March 2005.

[12] McCormick B.W. *Aerodynamics, Aeronautics & Flight Mechanics*. John Wiley & Sons, Inc., 1979.

[13] Michael Selig. *Summary of Low-Speed Airfoil Data*, volume 1. SoarTech Publications, Virginia Beach, VA, 1995.

[14] Michael Selig. *Summary of Low-Speed Airfoil Data*, volume 2. SoarTech Publications, Virginia Beach, VA, 1996.

[15] Michael Selig. *Summary of Low-Speed Airfoil Data*, volume 3. SoarTech Publications, Virginia Beach, VA, 1997.